

# Texture Evolution During Annealing in Warm-Rolled and Cold-Rolled Ti-IF Steel

Yan-hui Guo, Zhao-dong Wang, and Guo-dong Wang

(Submitted September 16, 2009; in revised form April 23, 2010)

The texture characteristics and the recrystallization mechanism during annealing in warm rolled and subsequently cold rolled Ti-IF steel have been investigated by x-ray diffraction and electron backscattered diffraction (EBSD). The results attained by x-ray show that texture changes little until the holding time reaches 4 h. After annealing for 4 h, the orientation density of  $\alpha$ -fiber reduces dramatically, but the orientation density of  $\gamma$ -fiber has no obvious change; however, the density of  $\{332\}\langle113\rangle$  component increases. The EBSD analysis shows that orientated-nucleation dominates during recrystallization, and the orientation of the nuclei includes  $\gamma$ -orientation as well as  $\{332\}\langle113\rangle$  component.

**Keywords**  $\gamma$ -orientation, recrystallization texture, Ti-IF steel sheet,  $\{332\}\langle113\rangle$

## 1. Introduction

Interstitial-free (IF) steel exhibits excellent deep drawability, high plastic strain ratio, high elongation, high hardening index, and low yield to tensile strength ratio (Ref 1). These advantages greatly enhance its application for automobile manufacturing.

In order to obtain high intensity of  $\{111\}$  recrystallization texture, final rolling in the ferrite region has been introduced in some hot strip mills. After hot rolling in the ferrite region, the texture of IF steel consists of  $\alpha$ -fiber ( $\langle110\rangle/\text{RD}$ ) and  $\gamma$ -fiber ( $\langle111\rangle/\text{ND}$ ), this texture is different from the relatively random texture of the austenized region. The cold rolling texture of ferritic-rolled IF steel also consists of  $\alpha$ -fiber ( $\langle110\rangle/\text{RD}$ ) and  $\gamma$ -fiber ( $\langle111\rangle/\text{ND}$ ), but after annealing, the recrystallization texture consists only of  $\gamma$ -fiber. The nature of  $\{111\}\langleuvw\rangle$ ; recrystallization texture of IF steel plays a significant role in determining the planar anisotropy of the sheet properties (Ref 2–5). This is particularly important to the deep drawability of steel sheets, so numerous experiments have been carried out to understand the mechanisms of recrystallization in IF steel (Ref 6–8).

The fundamental processes of static and dynamic recrystallization are nucleation and growth (Ref 9). Two main theories of recrystallization texture are currently accepted. The first one, oriented nucleation theory, assumes that nuclei of specific orientations form faster than those of other orientations, and consequently determine the recrystallization texture (Ref 10). The second one, oriented growth theory, claims that there exist

specific rotation relationships with rapid grain boundary migration. These specific relationships between deformed and recrystallization textures are about  $30^\circ\langle110\rangle$  for bcc metals (Ref 11).

This study investigates the recrystallization kinetics and the micro texture of nucleus. The aim of the study is to gain further insight into the mechanisms of the recrystallization texture of IF steel.

## 2. Experimental Procedures

The chemical composition of the steel studied in this study is given in Table 1. The hot band was cold rolled with 75% reduction using a two-high reduction mill. The aim of this work is to investigate the nucleation and its growth at the beginning of recrystallization, and so short holding time and low annealing temperature were employed. The annealing temperature was 600 °C, and the holding times were 0, 20, 50, 90, 150, and 240 min. After annealing, the samples were air cooled.

Texture measurements were conducted after hot rolling, cold rolling, and annealing by x-ray diffraction using a Philips X'PERT Pro system. Orientation distribution functions (ODF) of the global structure were calculated using the two-step method with  $l_{\max} = 16$  based on the series expansion method proposed by Roe (Ref 12) from three incomplete pole figures of  $\{200\}$ ,  $\{110\}$ , and  $\{211\}$  and expressed using  $\varphi = 45^\circ$  ODF sections. Experimental background and defocusing corrections were applied by measuring the texture of a pure iron random sample. In order to illustrate the presence of various textures, the so-called skeleton plots were constructed from the ODF data. These plots describe the preferred crystallographic orientations in the rolling direction ( $\text{RD}/\langle110\rangle$ ,  $\alpha$ -fiber), normal direction ( $\text{ND}/\{111\}$ ,  $\gamma$ -fiber) and transverse direction ( $\text{TD}/\langle110\rangle$ ,  $\varepsilon$ -fiber).

The metallographic photos and EBSD maps, which were taken on sections perpendicular to the transverse direction and annealed for different times, are given. EBSD maps were determined from the mid thickness region of the sheets using

Yan-hui Guo, Material Engineering Department, Shanghai Institute of Technology, Shanghai 200235, China; Zhao-dong Wang and Guo-dong Wang, The State Key Lab. of Rolling & Automation of Northeastern University, Shenyang 110004, China. Contact e-mail: gyh415@126.com.

a JEOL JSM-6500F SEM, coupled with an EBSD facility and Channel 5 software. For EBSD analysis, the specimens were mechanically polished and then electropolished in a solution of 1000 mL ethanol and 100 mL perchloric acid.

### 3. Results

The micrographs for the annealed sheets are shown in Fig. 1. When the annealing temperature reaches 600 °C, deformation bands are still the main characteristics of microstructure. With the holding time increasing to 20 min, it is obvious that some fine grains develop in the deformation bands. As the time increases to 50 min, more recrystallized grains form, and some of the grains begin to coarsen. With further increase in the holding time, the density of deformation bands gradually decreases. At the holding time of 4 h, only a few

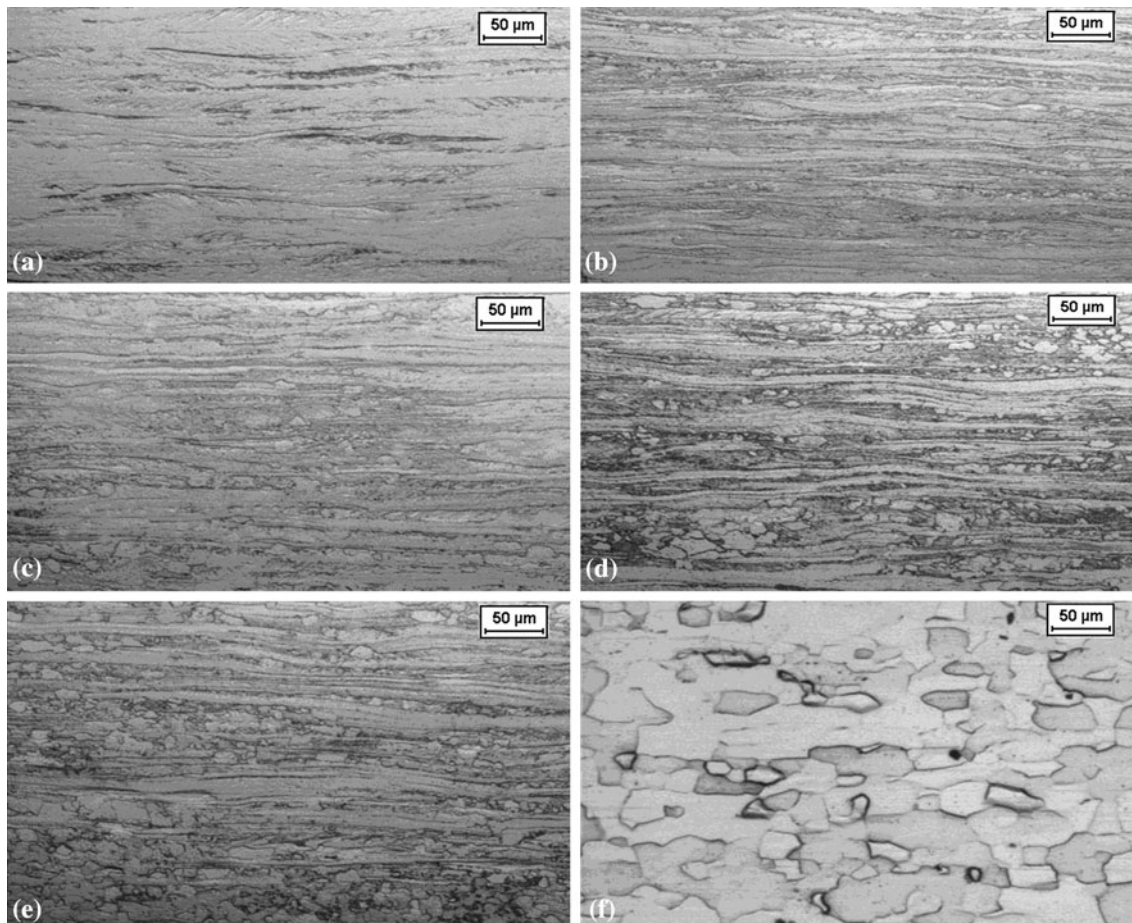
deformation bands are left, and much of the microstructure consists of fine grains.

Figure 2 shows the global texture of Ti-IF steel sheets annealed for different times. The texture obtained by x-ray has no obvious change until the annealing time reaches 4 h. After annealing for 4 h, the density of  $\alpha$ -fiber reduces dramatically, and the main texture component is  $\gamma$ -fiber ( $\langle 111 \rangle / \text{ND}$ ). This is consistent with Vandeschueren et al.'s (Ref 13) results. They have concluded that  $\gamma$ -oriented nuclei do not grow into the matrix until the end of recrystallization. Hence, texture change cannot be investigated after holding for a short time and until 4 h, and then the significant reduction of  $\alpha$ -fiber can just be investigated.

The orientation map and constant  $\varphi_2$ ODF sections obtained from the EBSD for Ti-IF steel annealed for 20 min are shown in Fig. 3. The orientation map of specific orientations for Ti-IF steel annealed for 20 min is shown in Fig. 4. As can be seen in the figure, the recrystallization grains are defined as the nearly

**Table 1 Chemical composition of the test steel (mass contents in %)**

Steel grade	C	Si	Mn	P	S	Ti	Nb	N	Als
Ti-IF steel	0.004	0.015	0.12	0.007	0.007	0.068	<0.005	0.0028	0.034



**Fig. 1** Metallographs of Ti-IF steel sheets annealed for different times (a) 0 min; (b) 20 min; (c) 50 min; (d) 90 min; (e) 150 min; and (f) 240 min

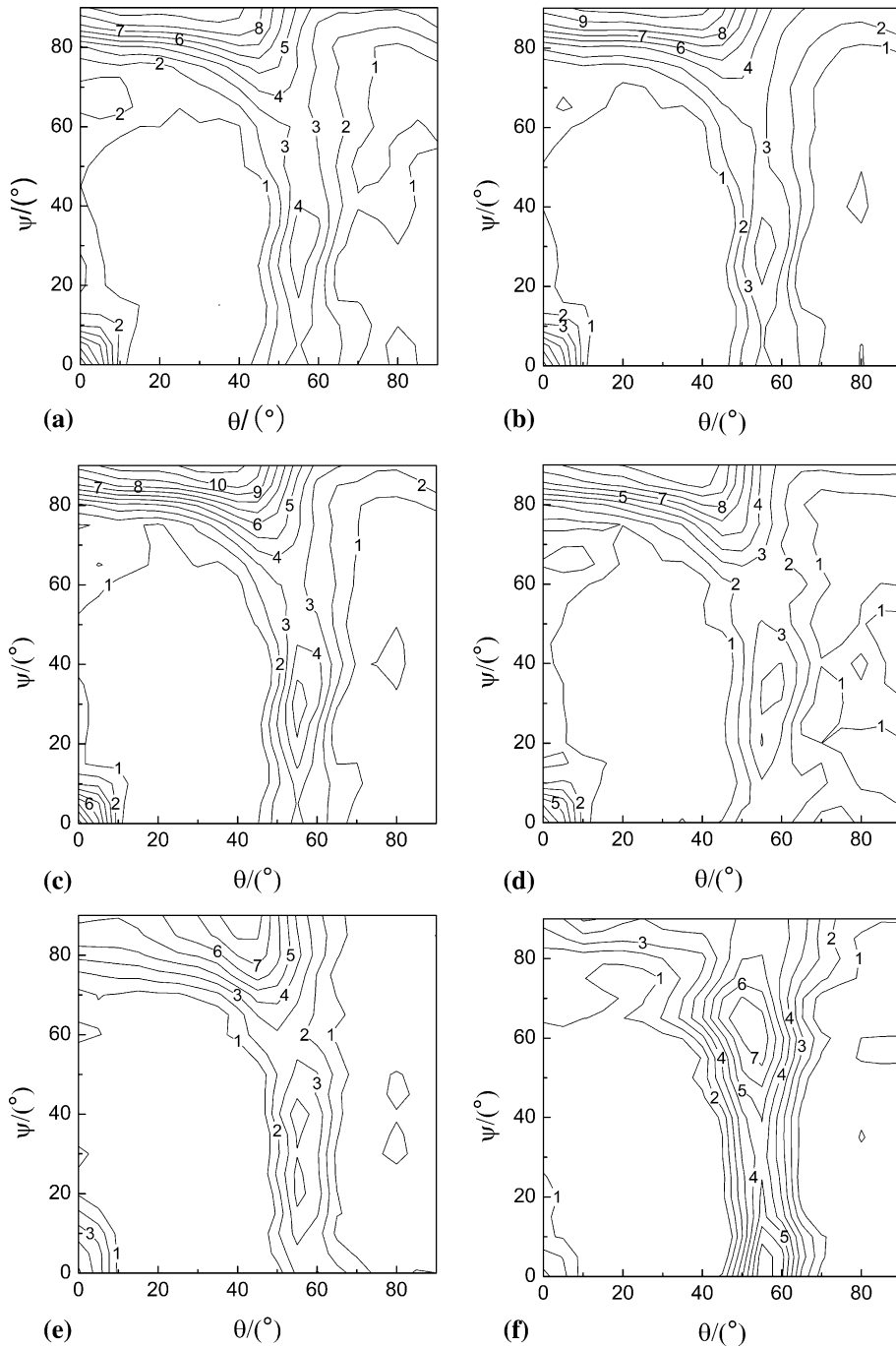
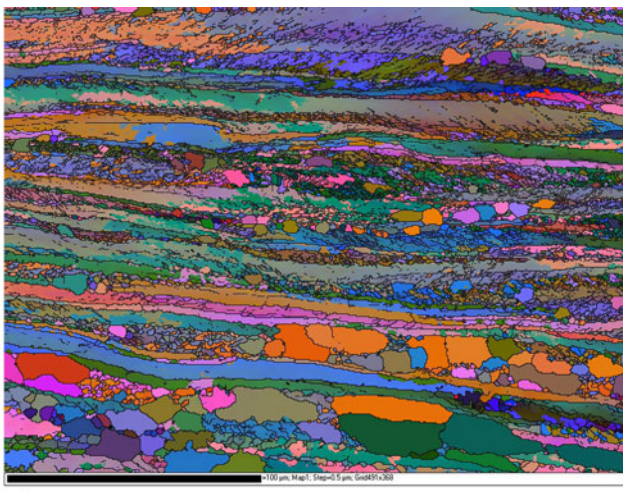


**Fig. 2**  $\phi = 45^\circ$  ODF section from x-ray of Ti-IF steel annealed for different times (a) 0 min; (b) 20 min; (c) 50 min; (d) 90 min; (e) 150 min; and (f) 240 min

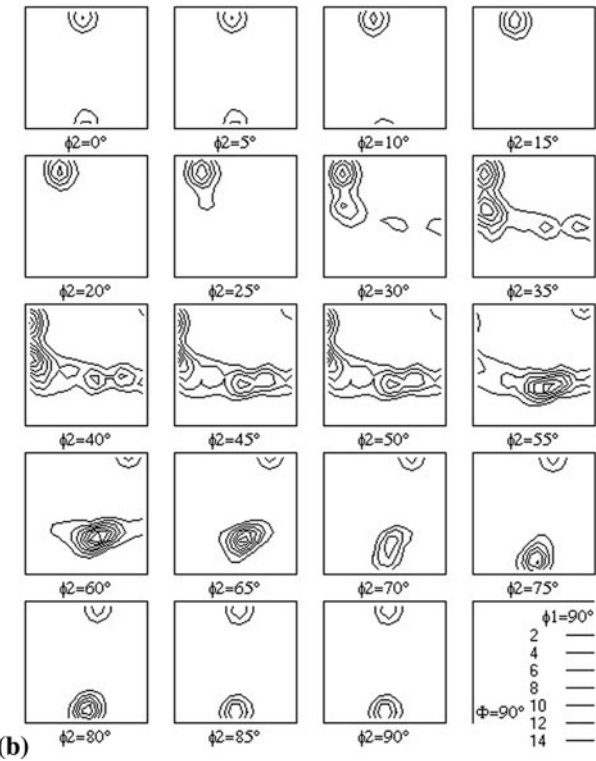
equiaxed areas which have clear kikuchi patterns, have misorientation with the neighboring region higher than  $15^\circ$ , and do not contain interior interfaces less than  $2^\circ$ ; others are considered to be deformation bands. The orientation color is described as the red belongs to  $\{001\}\langle110\rangle$  orientation, pink belongs to  $\{114\}\langle110\rangle$  orientation, yellow belongs to  $\{112\}\langle110\rangle$  orientation, blue belongs to  $\{111\}\langle112\rangle$  orientation, purple belongs to  $\{111\}\langle110\rangle$  orientation, and green belongs to  $\{332\}\langle113\rangle$  orientation. Other orientations are gray.

It can be seen from Fig. 3 and 4 that the recrystallized grains distribute non-homogeneously. Obviously, recrystallization

happens only in partial deformation bands. It can be seen from Fig. 4 that the orientations of the firstly formed nuclei are  $\{111\}\langle112\rangle$ ,  $\{111\}\langle110\rangle$ , and  $\{332\}\langle113\rangle$  which is close to  $\{111\}\langle112\rangle$ . Moreover,  $\{111\}\langle112\rangle$ -oriented nuclei formed in the  $\{111\}\langle110\rangle$ -oriented deformation bands, and  $\{111\}\langle110\rangle$ -oriented nuclei formed in the  $\{111\}\langle112\rangle$ -oriented deformation bands. The formation of  $\{332\}\langle113\rangle$ -oriented grains is caused by the fragmentation of  $\gamma$ -oriented deformation bands. When annealed at low temperature, the orientations of nuclei scans and  $\{554\}\langle225\rangle$ - $\{332\}\langle113\rangle$ -oriented nuclei come into being. The nuclei prefer to form in the  $\gamma$ -oriented deformation bands,



(a)



(b)

**Fig. 3** Orientation map and constant  $\phi_2$ ODF sections from EBSD for Ti-IF steel annealed for 20 min (a) orientation map; and (b) constant  $\phi_2$ ODF sections

and no nucleus is investigated in the  $\alpha$ -oriented deformation bands. It is found that nuclei easily form at the interface whose misorientation with the neighboring nuclei is higher than  $15^\circ$  in  $\gamma$ -oriented deformation bands, while in the single  $\gamma$ -oriented deformation bands, no nucleus is investigated.

The orientation map and constant  $\phi_2$ ODF sections of Ti-IF steel annealed for 90 min are shown in Fig. 5. More recrystallized grains form after annealing for 90 min, and some grains begin to grow. The nuclei consume their neighboring matrix and turn into elongated grains. Then, the grain boundaries bulge to the neighboring deformation bands, and equiaxed grains come into being. In addition, the growth rate of the nuclei is similar, and this proves that selective growth is not the main mechanism of the nuclei formation.

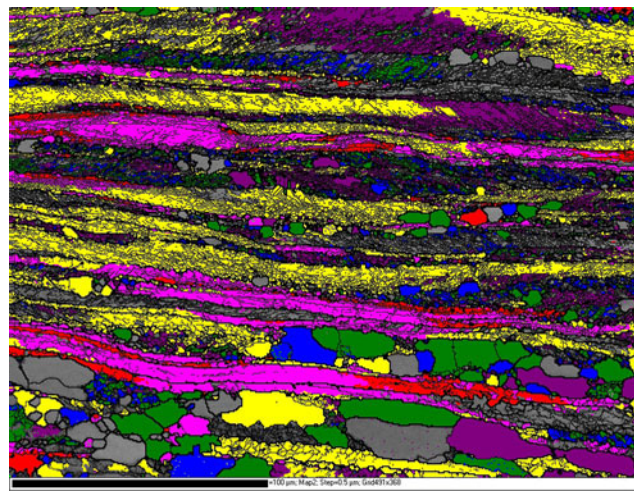
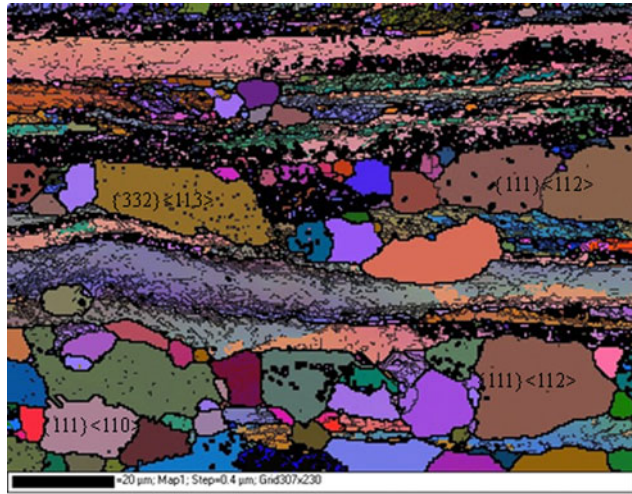


**Fig. 4** Orientation map for specific orientations for Ti-IF steel annealed for 20 min

The formation of the recrystallization texture is a competitive process between nucleation and growth. After annealing at  $600^\circ\text{C}$ , the main components are  $\{111\}\langle112\rangle$ ,  $\{111\}\langle110\rangle$ , and  $\{332\}\langle113\rangle$ ; this agrees with the main orientation of the nuclei. There is still a dispute about the recrystallization mechanism of IF steel. Supporters of the oriented nucleation theory believe that there is higher stored energy in the  $\gamma$ -orientation. During annealing, the subgrains with the  $\gamma$ -orientation nucleate first and determine the recrystallization texture. Supporters of the theory of the selective growth believe that the  $\gamma$ -oriented nuclei consume  $\{111\}\langle112\rangle$ -oriented matrix and strong  $\gamma$ -fiber form. Recently, more and more researchers have concluded that the recrystallization mechanism of IF steel is that of the oriented nucleation. In addition, the firstly formed  $\gamma$ -oriented nuclei can be explained from the standpoint of stored energy. The stored energy in deformed grains varies for different orientations. The stored energy changes in the following order:  $\{110\} > \{111\} > \{112\} > \{100\}$ . Although the stored energy of  $\{110\}$ -oriented is high, only a few  $\{110\}$ -oriented grains form during cold rolling. The recrystallized grains are those that nucleate rapidly and have a large quantity. Hence,  $\{110\}$ -oriented grains are fewer for the lack of quantity, and finally  $\{111\}$ -oriented grains dominate in the recrystallized grains.

At the beginning of recrystallization,  $\gamma$ -oriented nuclei and  $\{332\}\langle113\rangle$ -oriented nuclei develop in the  $\gamma$ -oriented deformation bands. At the late stage of recrystallization, as the  $\gamma$ -oriented recrystallized grains meet the  $\alpha$ -oriented deformation bands, the former will consume the latter.  $\{111\}\langle110\rangle$  and  $\alpha\text{-}\{112\}\langle110\rangle$  have the relationship of  $35^\circ\langle110\rangle$ , namely,  $\Sigma 9$  CSL.  $\{332\}\langle113\rangle$  and  $\alpha\text{-}\{112\}\langle110\rangle$  meet the relationship of  $27^\circ\langle110\rangle$ , namely,  $\Sigma 19a$  CSL.  $\{111\}\langle112\rangle$  and  $\alpha\text{-}\{001\}\langle110\rangle$  have  $54^\circ\langle110\rangle$  relationship, namely,  $\Sigma 11$  CSL. Hence,  $\{111\}\langle110\rangle$ -oriented recrystallized grain will grow into  $\{112\}\langle110\rangle$ -oriented deformation bands;  $\{111\}\langle112\rangle$ -oriented recrystallized grain will grow into  $\{001\}\langle110\rangle$ -oriented deformation bands;  $\{332\}\langle113\rangle$ -oriented recrystallized grain will grow into  $\{112\}\langle110\rangle$ -oriented deformation bands. As the recrystallization is complete, the recrystallization texture is that of mainly  $\gamma$ -fiber. It has been proved that the nuclei with low stored energy form at lower temperature and those with a high stored energy form at a higher temperature. Therefore, with increasing temperature,  $\gamma$ -oriented nuclei will increase and become sharp.



(a)

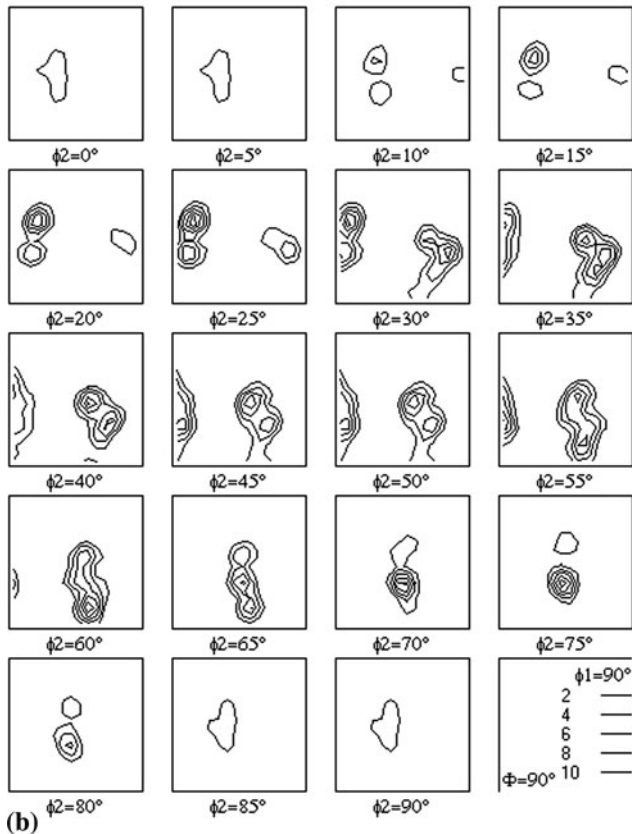


**Fig. 5** Orientation map and constant  $\phi_2$ ODF sections from EBSD for Ti-IF steel annealed for the 90-min (a) orientation map; (b) constant  $\phi_2$ ODF sections

## 4. Conclusions

When the annealing temperature is 600 °C, the reduced  $\alpha$ -fiber transforms to  $\gamma$ -fiber as well as  $\{332\}\langle113\rangle$  components at the late stage of recrystallization. The EBSD analysis shows that the orientated nucleation dominates during recrystallization, and the orientation of the nuclei includes  $\{332\}\langle113\rangle$  component besides the  $\gamma$ -orientation.

## Acknowledgment

The authors are grateful to the National Natural Science Foundation of China for financial support, under Grant No 50104004.

## References

- H. Zhao, S.C. Rama, G.C. Barber, Z. Wang, and X. Wang, Experimental Study of Deep Drawability of Hot Rolled IF Steel, *J. Mater. Process. Technol.*, 2002, **128**(1–3), p 73–79
- W.B. Hutchinson, Development and Control of Annealing Textures in Low-Carbon Steels, *Int. Met. Rev.*, 1984, **29**(1), p 25–42
- R.K. Ray, J.J. Jonas, and R.E. Hook, Cold Rolling and Annealing Textures in Low Carbon and Extra Low Carbon Steels, *Int. Mater. Rev.*, 1994, **39**(4), p 129–172
- H. Saitoh, K. Ushtoda, and T. Senuma, Structural and Textural Evolution During Subsequent Annealing of Steel Sheet Hot-Rolling in  $\alpha$  Phase, *THERMEC'88*, Iron and Steel Institute of Japan, Tokyo, 1988, p 628–635
- T. Nakamura and K. Esaka, Development of Hot Rolled Steel Sheet With High  $r$  Value, *International Conference on Physical Metallurgy of Thermo Mechanical Processing of Steels and Other Metals, THERMEC'88*, Iron and Steel Institute of Japan, Tokyo, 1988, p 644–651
- Y.B. Park, D.N. Lee, and G. Gottstein, A Model of the Development of Recrystallization Textures in Body Centered Cubic Metals, *Mater. Sci. Eng.*, 1998, **257**, p 178–184
- S.H. Choi, Simulation of Stored Energy and Orientation Gradients in Cold-Rolled Interstitial Free Steels, *Acta Mater.*, 2003, **51**, p 1775–1788
- M.R. Barnett and L. Kestens, Formation of  $\{111\}\langle110\rangle$  and  $\{111\}\langle112\rangle$  Textures in Cold Rolled and Annealed IF Sheet Steel, *ISIJ Int.*, 1999, **39**(9), p 923–929
- J. Baczyński and J.J. Joans, *Proc. ICOTOM 11*, Vol. 1, 1996, p 387
- R.D. Doherty, D.A. Hughes, F.J. Humphreys et al., Current Issues in Recrystallization, *Mater. Sci. Eng. A*, 1997, **238**(2), p 219–274
- F.J. Humphreys and M. Matherly, *Recrystallization and Related Annealing Phenomena*, Elsevier Science Ltd., New York, 1995, p 173–178
- R.Y.-J. Roe, Description of Crystallite Orientation in Polycrystalline Materials. III. General Solution to Pole Figure Inversion, *J. Appl. Phys.*, 1965, **36**(6), p 2024–2031
- D. Vandershueren, N. Yoshinaga, and K. Koyama, Recrystallization of Ti IF Steel Investigated with Electron Backscattering Pattern (EBSP), *ISIJ Int.*, 1996, **36**(8), p 1046–1054